Three-Dimensional Nonisothermal Simulation of a Coat Hanger Die

Tingqi Wu, Bo Jiang, Shuhua Xu, Nabin Huang

School of Mechanical and Electrical Engineering, Beijing University of Chemical Technology, Beijing 100029, People's Republic of China

Received 9 March 2005; accepted 1 October 2005
DOI 10.1002/app.23368
Published online in Wiley InterScience (www.interscience.wiley.com).

ABSTRACT: We studied the nonisothermal flow of Carreau fluid in a coat hanger die. A general three-dimensional finite volume code was developed for the purpose of flow analysis. The pressure distribution and velocity distribution were obtained in addition to the temperature distribution. The results illustrated that the highest temperature occurred more by the center of manifold than by the die-lip region. In the regions where the die gap was small relatively, the wall temperature played a key role in the determination of the temperature distribution in the melt. However, in the manifold, the viscous dissipation was the key factor that determined the temperature distribution in the melt where the heat conduction was relatively poor because of the thicker gap. © 2006 Wiley Periodicals, Inc. J Appl Polym Sci 101: 2911–2918, 2006

Key words: nonisothermal; simulation; coat-hanger die

INTRODUCTION

Coat hanger dies are used extensively for delivering wide uniform sheets of liquids in polymer processing industries. As we know, they provide a smooth, dead-spot, free-flow path and thus produce sheet without weld lines.[1] A large number of published articles have been devoted to the design and optimization of coat hanger dies. These articles can be put into two categories,[2] that is, analytical solution and numerical simulation. The analytical models were used for the initial determination of coat hanger geometries rather than for a precise description of flow inside a whole die. It is well known that no simple mathematical formula can be used to compute the flow regimes within a coat hanger die. Consequently, the analytical models were mainly used for one-dimensional or two-dimensional flow analysis. Numerical methods can be used, especially for dies with complicated geometries and for polymer melts with complex natures and physical properties. However, most published work related to numerical methods has focused on the introduction of methods used for die design and the description of comparisons of simulation results against experimental data.[3] Only a few recent publications have provided any detailed analyses of the flow field in pipe dies.[4] Huang et al.[3] gave a comprehensive three-dimensional (3-D) analysis of polymer melt flow in a coat hanger die with a commercially available package, FIDAP. However, in that article, the research was based on the isothermal flow, and the flow index (n) was set to be constant. In fact, the isothermal flow of polymer melts are difficult to achieve in engineering practice,[5] and n is dependent on the temperature.[6]

This research program has concentrated on a comprehensive analysis of polymer melt flow in a coat hanger die by means of 3-D computational fluid dynamics techniques. The polymeric liquid was nonisothermal, and the Carreau model was used to describe the rheological behavior of the polymer melt. The aim of this research was to provide a comprehensive understanding of the flow behavior of a polymer melt within a coat hanger die on which further optimization of die design can be based.

ANALYSIS

The polymer melt flow in a coat hanger die was examined by means of 3-D computational fluid dynamics techniques. A schematic of the die considered here is shown in Figure 1. The flow simulation was full 3-D and nonisothermal. Hence, the momentum and energy conservation equations were coupled through temperature-dependent constitutive equations. In the numerical analysis of extrusion dies, the Carreau models were used with consideration of its better representations of the entire viscosity (η) curve. The temperature-shifting function was used to illustrate the temperature influence on the rheological aspects of polymer fluid.

Correspondence to: T. Wu (wutingqi@sohu.com).

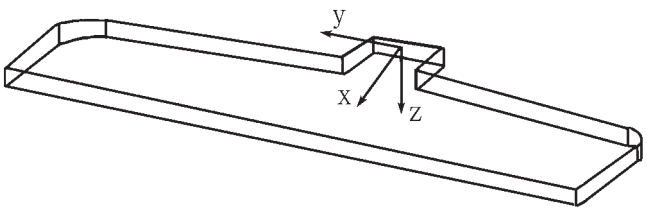

Figure 1 Schematic of a coat hanger die.

THEORETICAL DEVELOPMENTS

Nonisothermal modeling of polymer melt

The general 3-D fluid motion in a coat hanger die is considered here, and a Cartesian coordinate system (x,y,z) can be introduced to such die. The flow through extrusion die for an incompressible fluid, such as a polymer melt, is governed by the usual conservation equations of mass, momentum, and energy, that is

$$\nabla \underline{\mathbf{v}} = 0 \tag{1}$$

$$-\nabla p + \nabla \underline{\underline{\tau}} = 0 \tag{2}$$

$$\rho C_p \underline{\mathbf{v}} \cdot \nabla T = k_d \nabla^2 T + \underline{\underline{\tau}} : \nabla \underline{\mathbf{v}} \tag{3}$$

where $\underline{\mathbf{v}}$ is the velocity vector, p is the scalar pressure, $\underline{\underline{\tau}}$ is the extra stress tensor, ρ is the density, C_p is the heat capacity, k_d is the thermal conductivity, and T is the temperature.

$\underline{\mathbf{v}}$ is expressed as

$$\underline{\mathbf{v}} = u\underline{\mathbf{i}} + v\underline{\mathbf{j}} + w\underline{\mathbf{k}} \tag{4}$$

where u, v, w are velocity components in x, y, z direction, respectively, i, j, k are the unit vector in x, y, z direction and the shear stress ($\underline{\underline{\tau}}$) is defined as

$$\underline{\underline{\tau}} = \eta(\dot{\gamma})(\nabla \underline{\mathbf{v}} + \nabla \underline{\mathbf{v}}^T) \tag{5}$$

Constitutive equation

A fully 3-D analysis requires a continuous η correlation that extends from zero shear rate all the way to the highest shear rate that may occur in a die, such as at the walls of the die.[7] Hence, the Carreau model was used as a better representation of the entire η curve.[7,8] To reflect the influence of nonisothermal effects on the rheological behavior of polymer melt, the temperature-shifting function was introduced. The nonisothermal constitutive equation used here can be expressed as

$$\eta = \eta_0[1 + (\lambda\dot{\gamma})^2]^{\frac{n-1}{2}} \exp\left[\frac{E_0}{R_0}\left(\frac{1}{T} - \frac{1}{T_0}\right)\right] \tag{6}$$

where λ is the time constant.

The value of local shear rate ($\dot{\gamma}$) is calculated by

$$\dot{\gamma} = (\underline{\underline{\dot{\gamma}}} : \underline{\underline{\dot{\gamma}}}/2)^{1/2} \tag{7}$$

where $\underline{\underline{\dot{\gamma}}}$ is the shear rate tensor.
with the following equation

$$\underline{\underline{\dot{\gamma}}} = \nabla \underline{\mathbf{v}} + \nabla \underline{\mathbf{v}}^{\mathbf{T}} \tag{8}$$

where η_0 is the viscosity at shear rates ($\dot{\gamma}$'s) approaching zero, γ is the relaxation time obtained from the η curve of the material, E_0 is the activation energy constant, R_0 is the ideal gas constant, and T_0 is a reference temperature. E_0 was determined from η_0 data.[9] n was assumed to be dependent on the temperature through the following expression, which could be derived from experimental data:

$$n(T) = \frac{T}{a} + b \tag{9}$$

where a and b are constant.

Boundary conditions

The solution of eqs. (1)–(3) for the three components of velocity and the pressure throughout a die require specifying boundary conditions. At both the die inlet and outlet, fully developed flow is assumed, that is

$$\partial u/\partial x = 0 \text{ and } v = w = 0 \tag{10}$$

where the coordinate x is taken in the extrusion direction.

The problem considered here has a plane of symmetry at $y = 0$. In such case, one can take advantage of this symmetry to halve the domain by imposing symmetry boundary condition on the plane, that is

$$v = \partial u/\partial y = \partial w/\partial y = 0 \tag{11}$$

Similarly, there is a second symmetry plane at $z = 0$ where

$$w = \partial u/\partial z = \partial v/\partial z = 0 \tag{12}$$

No slip is assumed on all die surfaces, that is

$$\underline{\mathbf{v}} = 0 \tag{13}$$

For the thermal boundary conditions, we may have a constant temperature profile at the die entrance and a constant wall temperature.

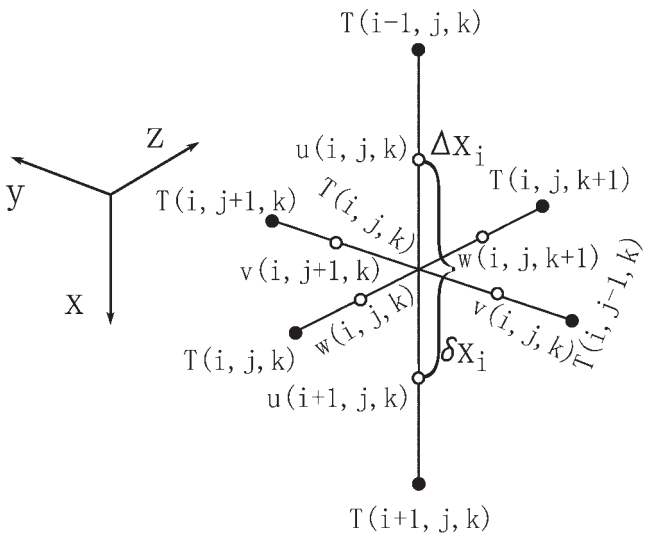

Figure 2 Diagram of temperature distribution on the staggered grid.

Method of solution

The previous constitutive equation was solved together with the conservation equations with the finite volume method with the unknown velocities, pressure, and temperature, and the central difference technique was used to determine the governing equations. To avoid the nonsensical pressure distribution resulting from the central difference formulation for the pressure gradients, a staggered grid technique was adopted here. Then, the SIMPLE algorithm was used to calculate the velocity and pressure fields. Details of the program about the discrete technique mentioned here are discussed elsewhere.[10–14]

The expression of energy [eq. (3)] under the Cartesian coordinate system is

$$\rho C_v\left(u\frac{\partial T}{\partial x}+v\frac{\partial T}{\partial y}+w\frac{\partial T}{\partial z}\right)=k_d\left[\frac{\partial^2 T}{\partial x^2}+\frac{\partial^2 T}{\partial y^2}+\frac{\partial^2 T}{\partial z^2}\right]+\eta\dot{\gamma}^2. \quad (14)$$

where C_v is specific heat.

To compute the temperature field, it is necessary to discretize eq. (14) on the staggered grid shown in Figure 2.

The discrete expression of T in x direction centered the node (i,j,k) is given as

$$(a_{i-1}+a_{i+1})T(i,j,k)=a_{i-1}T(i-1,j,k)+a_{i+1}T(i+1,j,k) \quad (15)$$

with

$$a_{i-1}=a_{i-1,1}+a_{i-1,2} \quad (15a)$$

$$a_{i+1}=a_{i+1,1}-a_{i+1,2} \quad (15b)$$

$$a_{i-1,1}=\frac{k_d}{\Delta x_i \delta x_i} \quad (15c)$$

$$a_{i-1,2}=\frac{\rho C_v u(i,j,k)}{2\Delta x_i} \quad (15d)$$

$$a_{i+1,1}=\frac{k_d}{\Delta x_{i+1}\delta x_i} \quad (15e)$$

$$a_{i+1,2}=\frac{\rho C_v u(i+1,j,k)}{2\Delta x_{i+1}} \quad (15f)$$

where Δx_i is the spacing between the grid point (i,j,k) and the grid point $(i-1,j,k)$ in the x direction. In a similar vein, Δx_{i+1} is defined as the spacing between grid point (i,j,k) and the grid point $(i+1,j,k)$, and δx_i is the half-spacing between grid point $(i-1,j,k)$ and the grid point $(i+1,j,k)$. To reflect the influence of heat convection and conduction to temperature field, the Peclet number (Pe) was used here, which represents the ratio of heat convection to conduction:

$$Pe_l=\frac{a_{l,2}}{a_{l,1}} \qquad (l=i-1,i+1) \quad (16)$$

where l is defined as a variable, which is equal to $i-1$ or $i+1$.

According to the magnitude of Pe, Patankar[15] provided a simple method to determine the coefficient of temperature in eq. (15), which is demonstrated next.

In the case of $l=i-1$

$$\begin{array}{ll} Pe_l<-10 & a(i-1,j,k)=0 \\ -10\le Pe_l\le 0 & a(i-1,j,k)=(1+0.1Pe_l)a_{l,1} \\ 0\le Pe_l\le 10 & a(i-1,j,k)=[(1-0.1Pe_l)^5+Pe_l]a_{l,1} \\ Pe_l>10 & a(i-1,j,k)=a_{l,2} \end{array} \quad (17a)$$

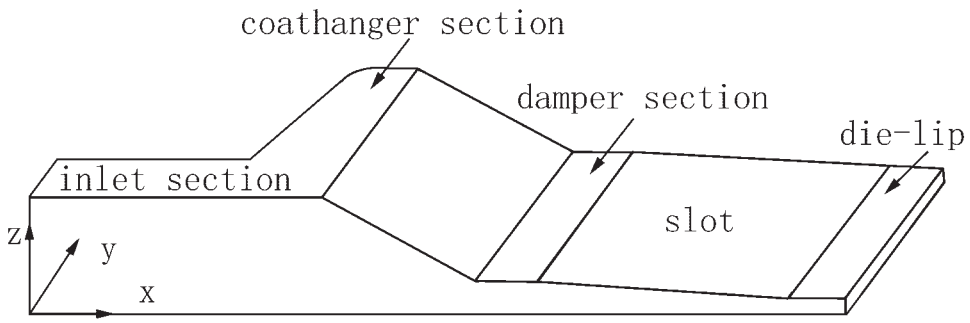

Figure 3 Diagram of a quarter of a coat hanger die.

and in the case of $l = i + 1$

$$\begin{array}{ll} Pe_l < -10 & a(i+1,j,k) = -a_{l,2} \\ -10 \le Pe_l \le 0 & a(i+1,j,k) = [(1+0.1Pe_l)^5 - Pe_l]a_{l,1} \\ 0 \le Pe_l \le 10 & a(i+1,j,k) = (1-0.1Pe_l)a_{l,1} \\ Pe_l > 10 & a(i+1,j,k) = 0 \end{array} \quad (17b)$$

Then eq. (15) can be rewritten as

$$[a(i-1,j,k) + a(i+1,j,k)]T(i,j,k) = a(i-1,j,k) \times T(i-1,j,k) + a(i+1,j,k)T(i+1,j,k) \quad (18)$$

Similarly, we obtained the corresponding coefficient of temperature in the y and z directions, and then, the discrete expression of eq. (15) was given:

$$AT(i,j,k) = a(i-1,j,k)T(i-1,j,k) + a(i+1,j,k)T \times (i+1,j,k) + b(i,j-1,k)T(i,j-1,k) + b(i,j+1,k)T \times (i,j+1,k) + c(i,j,k-1)T(i,j,k-1) + c(i,j,k+1)T \times (i,j,k+1) + \eta(i,j,k)\dot{\gamma}^2(i,j,k) \quad (19a)$$

where A to C represents the coefficient of temperature.

With the following equation:

$$A = a(i-1,j,k) + a(i+1,j,k) + b(i,j-1,k) + b(i,j+1,k) + c(i,j,k-1) + c(i,j,k+1) \quad (19b)$$

η and $\dot{\gamma}$ at the grid point (i,j,k) can be calculated with eqs. (6) and (7), respectively.

Solution procedure

A finite volume method was used to mesh the flow domain. Equations (1) and (2) were first solved for the three components of velocity and the pressure at the grid points under the specified boundary conditions and specified η field. Then, eq. (6) was used to calculate the η field with the assumed temperature field and known velocity gradients. After both the flow field and η field convergence, eq. (15) was then solved to obtain the temperature field. The process was repeated until convergence was reached. The iterative procedure was carried out as the following steps:

1. The fields of velocity and pressure were computed by solution of the momentum and continuity equations with the specified fields of η and temperature.
2. The field of η was computed with the known velocity gradients.
3. We repeated steps 1 and 2 until convergence was reached.
4. The field of temperature was computed with eq. (15)
5. Steps 1–4 were repeated until convergence was reached.

When solving the fields of temperature and flow, we found it necessary to proceed carefully and use underrelaxation factors. The underrelaxation factors for the calculation of η field and temperature field were 0.7 and 0.1, respectively. Values much higher resulted in growing oscillations of the η and temperature fields.

SIMULATION RESULTS AND ANALYSIS

The coat hanger die studied here had a manifold with a rectangular cross-section. Because of the symmetry, only a quarter of the whole die was simulated in the computer modeling, which is shown in Figure 3. Figure 4 shows the developed mesh of finite volume. There were a total of 33,693 grid points corresponding to 29,280 control volumes.

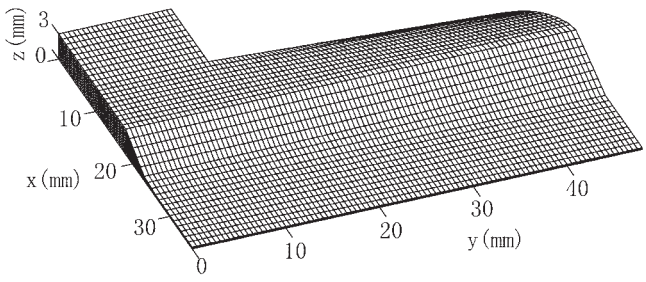

Figure 4 Mesh of finite volume for a quarter of coat hanger die.

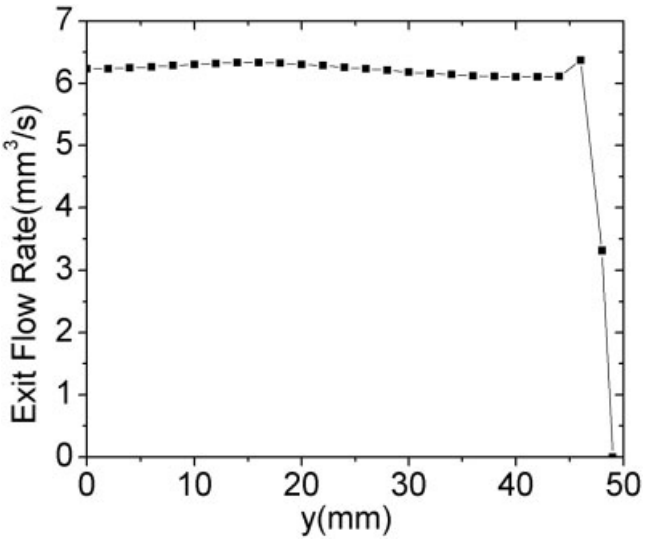

Figure 5 Exit flow distribution from the die.

The properties of material polystyrene (PS) used here are presented in Table I. The values were collected from Demay et al.'s[6] article. The relaxation time parameters were obtained from direct rheological measurements. The inlet temperature was set at 473 K, and the volumetric flow distribution at the exit of the die is plotted in Figure 5. Except for the side of the die, the flow uniformity was acceptable.

To investigate the flow behavior of the polymer melt inside the coat hanger die, we plotted $\underline{\mathbf{v}}$'s on the $x - y$ plane in Figure 6, where the arrowhead indicates the direction of velocity and the length of the stem indicates the magnitude of $\underline{\mathbf{v}}$. The thickness components vanish in this plane. As shown in the $\underline{\mathbf{v}}$ plot, the flow behavior of the polymer melt at the surface of symmetry was visible. In the entrance region, the polymer melt mainly flowed along the x direction. However, once arriving at the manifold region, the polymer melt flowed along the manifold mainly, and the velocity along the manifold decreased. From the arrow shown in Figure 6, we know that the transverse components initially developed around the neck, weakened gradually in the damper region and slot region, and eventually vanished in the die-lip region, where only the axial components existed. Figure 7 shows the $\underline{\mathbf{v}}$'s in the $x - z$ plane, which was the side view of the coat hanger die. The transverse components vanished in this plane. The development of the thickness components paralleled that of the transverse components. The thickness components also vanished in the die-lip region, and the parabolic profile could be clearly seen for the axial components in this region.

Figure 8 gives the isobars at the $x - y$ plane with inlet and wall temperatures of 473 K. At the entrance of manifold, the pressure was much greater than that at the end of manifold. This also indicated why the polymer melt flowed mainly along the manifold direction once it entered into the manifold section from the entrance of the die. As also shown in Figure 8, in those sections of manifold and damper, the pressure was always higher at $y = 0$, which was the die center, than in the side of the die. The slot section was the transition region, and the pressure distribution gradually flattened out as the polymer stream flowed down the channel. Hence, we know that before the die-lip region was entered, there were always flows from the center of the die to its far end. This flow was helpful for uniform distribution of exit flow rate. The contour line at the entrance of die lip was fairly parallel to the die exit width at the edge area of the die. This also indicated that a relatively uniform flow at the die edge was predicted.

In this study, we assumed the wall temperature to be constant, and the inlet temperature was set at 473 K. Figures 9 and 10 present the temperature field plotted on the $x - y$ surface with constant wall temperatures of 473 and 493 K, respectively. In these two cases, the predicted highest temperature was at the center of manifold region, not in the die-lip region. This seemed to be suspicious. Generally speaking, in the die-lip region, the shear rate is highest, and so is temperature. However, by the center of manifold, the heat conduction was relatively weak because of the

TABLE I
Material Properties

Material	ρ (kg/m^3)	Specific heat (J g^{-1} K^{-1})	η_0 (Pa s)	a (K^{-1})	E/R (K)	T_0 (K)	b	Conductivity (W m^{-1} K^{-1})	Relaxation time
PS	1040	1.9	19,860	−576	3200	473	1.6	0.17	0.28

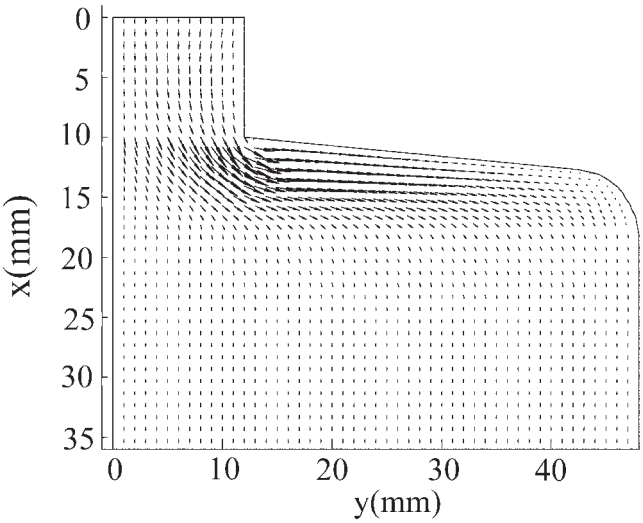

Figure 6 Velocity distributions at the $x - y$ surface of a quarter of the coat hanger die.

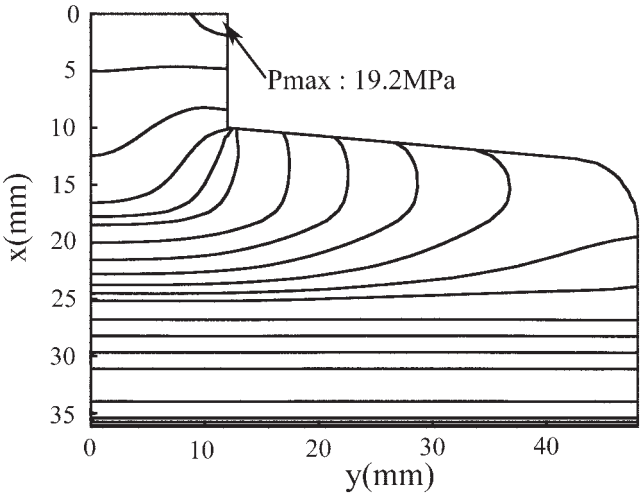

Figure 8 Isobars at the $x - y$ surface of a quarter of the coat hanger die.

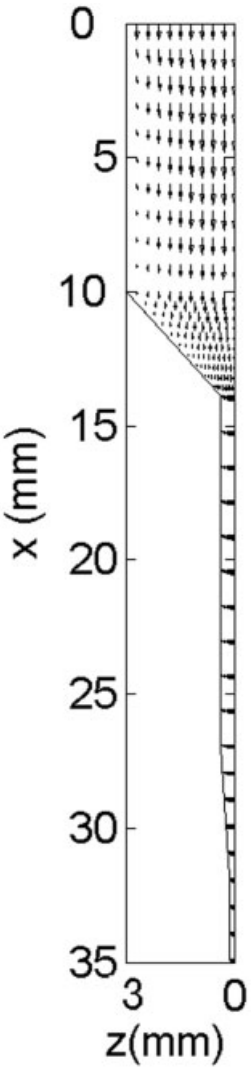

Figure 7 Velocity distributions at the $x - z$ plane of a quarter of the coat hanger die.

thicker gap. Hence, the viscous dissipation made the temperature in the melt rise significantly. Figures 11 and 12 show the corresponding temperature distributions on the $x - z$ surface of the coat hanger die. From the temperature distribution on the side view of the coat hanger die, we know that in the manifold in the transition region near the die wall, the temperature was higher than that near the $x - y$ plane. This was because of the higher shear rate. When the wall temperature was 473 K, from the damper region along the machine direction, the temperature in the melt decreased gradually. Eventually, in the die-lip region, the temperature in the melt approached the wall temperature because the opening of the slit was only 0.25 mm. As a comparison, when the wall temperature was 493 K, from the damper section along the machine direction, the temperature in melt increased gradually

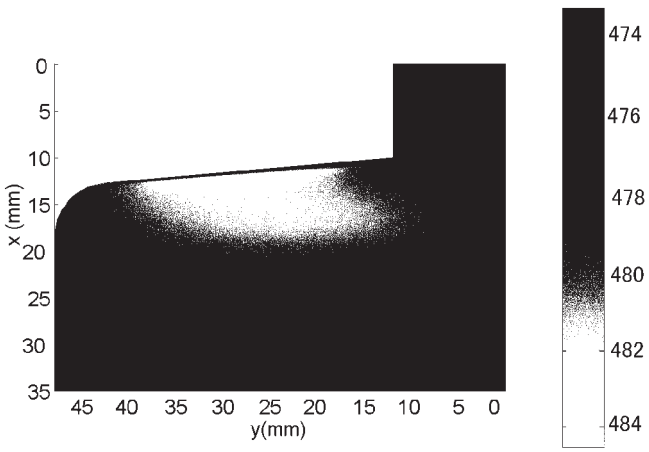

Figure 9 Temperature distributions at the $x - y$ surface of a quarter of the coat hanger die with inlet and wall temperatures of 473 K.

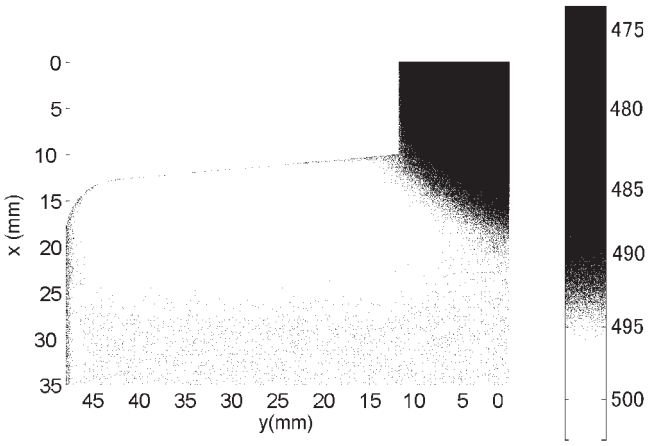

Figure 10 Temperature distributions at the $x - y$ surface of a quarter of the coat hanger die with an inlet temperature of 473 K and a wall temperature of 493 K.

because of the powerful heating of the die wall. Hence, in the manifold, the viscous dissipation, other than heat conduction, played a key role in the determination of the temperature distribution in the melt because of the thicker gap. However, in other regions in the die, the wall temperature had a key effect on the polymer melt distribution.

CONCLUSIONS

A procedure for analyzing the behavior of nonisothermal viscous polymer melt flow in a coat hanger die was carried out. The velocity field, pressure field, and temperature field on the symmetry planes were plotted. The results illustrate that the highest temperature occurred by the center of manifold due to the combined effects of viscous dissipation and heat convection rather than by the die-lip region.

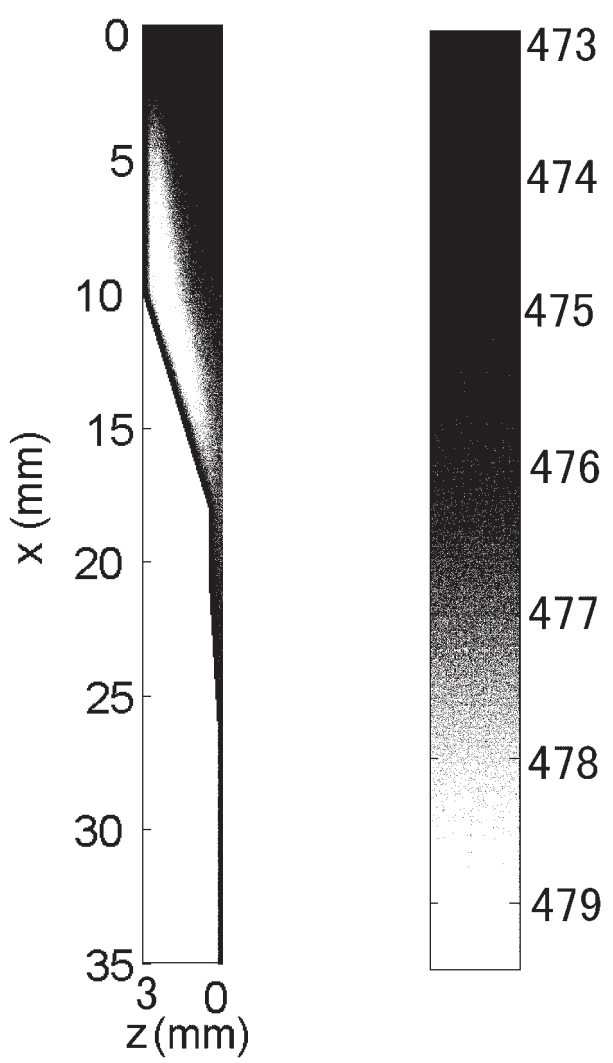

Figure 11 Temperature distributions at the $x - z$ surface of a quarter of the coat hanger die with inlet and wall temperatures of 473 K.

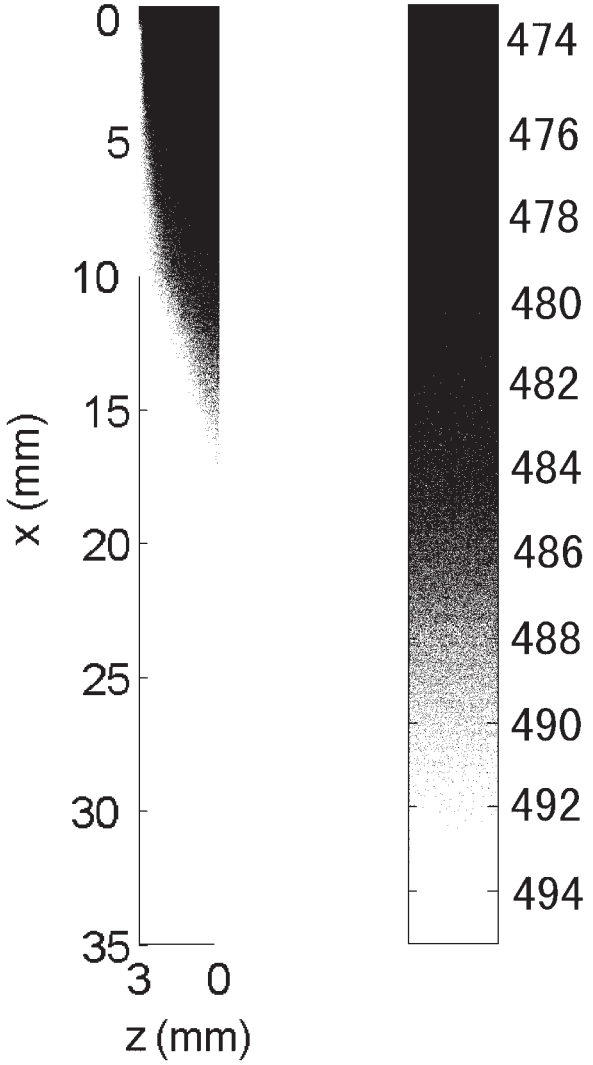

Figure 12 Temperature distributions at the $x - z$ surface of a quarter of the coat hanger die with an inlet temperature of 473 K and a wall temperature of 493 K.

The result predicted here is important for the processing of heat-sensitive materials, for instance, poly(vinyl chloride). Generally speaking, the temperature in the die lip is considered to be highest due to the higher shear rate. Hence, controlling the temperature in the die lip in an acceptable range is the key measure for ensuring the extrudate quality in processing the heat-sensitive materials; however, the temperature in the die lip was not the highest in the simulation presented here. Even when the temperature in the die lip is controlled in a suitable range, the relatively higher temperature in the manifold may still cause degradation of the processed material. In the regions where the die gap is relatively small, the wall temperature plays a key role in the determination of the temperature distribution in the melt. Obviously, being full 3-D and nonisothermal, the computer model should be much closer to the reality than those one or two nonisothermal simulations of a coat hanger die mentioned previously.

References

1. Matsubara, Y. Polym Eng Sci 1988, 28, 1275.
2. Sander, R.; Pittman, J. F. T. Polym Eng Sci 1996, 36, 1972.
3. Huang, Y. H.; Gentle, C. R.; Hull, J. B. Adv Polym Tech 2004, 23, 111.
4. Huang, Y.; Prentice, P. Polym Eng Sci 1998, 38, 1506.
5. Barakos, G.; Mitsoulis, E. J. Non-Newtonian Fluid Mech 1996, 62, 55.
6. Puissant, S.; Vergnes, B.; Demay, Y.; Agassant, J. F. Polym Eng Sci 1992, 32, 213.
7. Gifford, W. A. J Reinforced Plast Compos 1997, 16, 661.
8. Arpin, B.; Lafleur, P. G.; Sanschagrin, B. Polym Eng Sci 1994, 34, 657.
9. Meissner, J. Pure Appl Chem 1975, 42, 551.
10. Mei, R. W.; Plotkin, A. AIAA J 1986, 24, 1106.
11. Roahe, P. J Comput Fluids 1975, 3, 179.
12. Kuehn, T. H.; Goldstein, R. J. J Fluid Mech 1976, 74, 695.
13. Patankar, S. V.; Spalding, D. B. Int J Heat Mass Transfer 1972, 15, 1787.
14. Patankar, S. V. Numer Heat Transfer 1981, 4, 409.
15. Barakat, H. Z.; Clark, J. A. Procedings of Third International Heat Transfer Conference 1996, 2, 152.